# ESTIMATION OF PHASE SYNCHRONY USING THE SYNCHROSQUEEZING TRANSFORM

*Alireza Ahrabian and Danilo P. Mandic*

Imperial College London
Electrical and Electronic Engineering
Email: {alireza.ahrabian06, d.mandic}@imperial.ac.uk

**ABSTRACT**

Phase synchronization has emerged as an important concept in quantifying interactions between dynamical systems. In this work a robust estimate of the phase synchrony between bivariate signals is presented. This is achieved by extending the recently introduced synchrosqueezing transform (SST), a method that belongs to the class of reassignment techniques that generates highly localized time-frequency representations, so as to cater for bivariate data. The proposed method is shown to generate accurate estimates of phase synchrony on both synthetic and real world signals.

***Index Terms*—** Synchrosqueezing transform, phase synchronization.

## 1. INTRODUCTION

Analyzing the interactions between bivariate oscillatory systems is important in fields ranging from computational neuroscience [1] to oceanography [2]. Quantifying such interactions has traditionally been carried out using cross-correlation and coherence based techniques, however such methods assume linearity in the underlying systems and are therefore unable to capture the non-linear dynamics of real-world systems, such as interactions between cognitive processes [3] [4]. Recently, it has emerged that the interdependencies between weakly interacting oscillatory systems [5] [6] can be measured by estimating the phase synchrony that arises between such systems, a case where traditional methods fail. This has enabled real world applications of phase synchronization in the analysis of human physiological responses, such as in electroencephalography (EEG) [1] [3] and electromyography (EMG) data analysis [5].

Conventional phase synchrony estimation techniques are based on the Hilbert and wavelet transforms [1]; however the wavelet transform projects the signal across a fixed set of basis functions and has a limited time-frequency resolution, while using the Hilbert transform requires a narrowband signal, a rather stringent assumption. This affects the performance, as e.g. to produce monocomponent data filter cutoffs need to be determined a priori, thus prohibiting the tracking of drifting oscillations.

It has been demonstrated [7] that the empirical mode decomposition (EMD) overcomes such limitations, by decomposing a signal into a set of narrowband AM/FM components termed intrinsic mode functions (IMFs). This makes possible the application of the Hilbert transform to such well defined IMFs, in order to obtain an accurate estimate of instantaneous phase. In this way, the phase synchrony for all IMFs between the source pairs can then be calculated [8], however, the use of the univariate EMD on separate data channels does not guarantee the same number of IMFs across the data channels and the integrity of information. A rigorous way for EMD based phase synchrony was introduced in [9], by employing the bivariate empirical mode decomposition (BEMD) [10], which guarantees coherent and aligned bivariate IMFs, a prerequisite for accurate synchrony estimation.

While multivariate EMD-based phase synchrony methods have overcome the limitations of the traditional phase synchrony estimation techniques [9] [11] [12], a strong theoretical description for the underlying algorithms [13] is still lacking. To this end, we propose to apply the recently developed synchrosqueezing transform in estimating phase synchrony. The synchrosqueezing transform [13] [14] initially emerged as a post-processing technique to address limitations of the continuous wavelet transform (CWT) in simultaneously localizing oscillations both in time and frequency. By reassigning the energies of the CWT coefficients, such that the resulting energy of coefficients is concentrated around the instantaneous frequency curves of the oscillations, the synchrosqueezing transform has been shown to generate well localized time-frequency representations [15] [16].

In this work we propose a multivariate extension of the SST in order to identify bivariate monocomponent signals necessary for accurate estimation of the phase synchrony. The localization and stability of the proposed method is demonstrated on synthetic and real-world data.

## 2. SYNCHROSQUEEZED TRANSFORM

The continuous wavelet transform is a projection based time-frequency algorithm that finds signal components through a series of localized filters known as wavelets. A wavelet $\psi(t)$ is a square integrable function, and can be seen as set of scaled

978-1-4799-2893-4/14/$31.00 ©2014 IEEE

bandpass filters, that is convolved with a signal $x(t)$, as follows

$$W(a,b) = \int a^{-1/2}\psi\left(\frac{t-b}{a}\right)x(t)\,dt \tag{1}$$

where $W(a,b)$ are the wavelet coefficients. The scale factor $a$ shifts the wavelet $\psi(t)$ in the frequency domain so that oscillatory features across different frequency scales are captured. Given a sinusoid at a frequency $\omega_s$, the resulting CWT coefficients of the sinusoid will spread out around the scale factor $a_s = \frac{\omega_\psi}{\omega_s}$, where $\omega_\psi$ is the wavelet center frequency. In this way, the estimated instantaneous frequency present in the scales near the vicinity of $a_s = \frac{\omega_\psi}{\omega_s}$ is equal to the original frequency $\omega_s$. It is now possible, given an estimate of the instantaneous frequency $\omega_x(a,b)$

$$\omega_x(a,b) = -iW(a,b)\,\frac{\partial W(a,b)}{\partial b} \tag{2}$$

for each scale-time pair $(a,b)$, for the wavelet coefficients containing the same instantaneous frequencies to be combined in a procedure known as synchrosqueezing [13]. For the wavelet coefficients $W(a,b)$, the synchrosqueezing transform[1] $T(\omega,b)$ is given by

$$T(\omega_l,b) = \sum_{a_k:\,|\omega_x(a_k,b)-\omega_l|\le\Delta\omega/2} W(a_k,b)\,a^{-3/2}\,\Delta a_k \tag{3}$$

and it reallocates the energy of wavelet coefficients so as to enhance frequency localization.

## 3. PHASE SYNCHRONIZATION

For two oscillatory systems with instantaneous phases $\phi_x(t)$ and $\phi_y(t)$, the phase synchronization of the system is characterized by an index that measures the strength of phase locking that occurs between the difference of the instantaneous phases, $\phi_{xy}(t) = \phi_x(t) - \phi_y(t)$, that is $|\phi_{xy}(t)| < constant$. The phase synchrony index $\rho(t)$, used in this work is based on Shannon entropy [5] and is given by

$$\rho(t) = \frac{H_{max} - H}{H_{max}} \tag{4}$$

where $H = -\sum_{n=1}^{N} p_n \ln p_n$, is the entropy of the distribution of the windowed phase difference $\phi_{xy}(t - \frac{W}{2} : t + \frac{W}{2})$, for a given window length $W$, and $H_{max} = \ln N$ (where $N$ is the number of bins), is the maximum entropy within the window $W$, corresponding to a uniform distribution. It then follows that for a pair of systems that are in synchrony, the distribution of the phase difference will approach a Dirac delta distribution, and will thus have a low entropy and by (4) a high phase synchrony score.

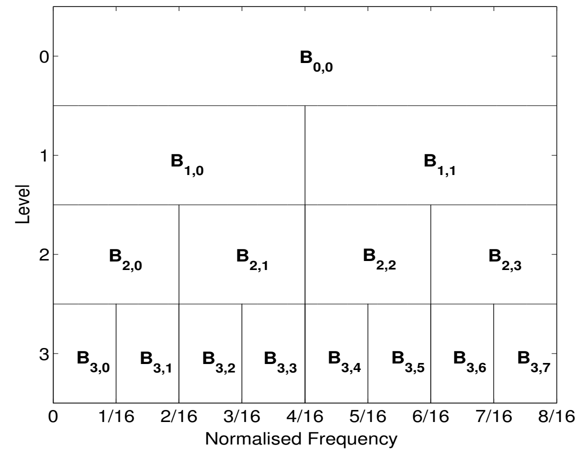


**Fig. 1**: The partitioned frequency domain with the multivariate bandwidth given by $\mathbf{B}_{l,m}$, where $l$ corresponds to the level of the frequency band ($L = 5$ typically), and $m$ is the frequency band index.

## 4. PHASE SYNCHRONIZATION USING SST

In order to measure the phase synchrony between two signals $x_1(t)$ and $x_2(t)$ the synchrosqueezing transform is first applied to each signal separately yielding the respective SST coefficients $T_1(\omega,b)$ and $T_2(\omega,b)$. Next, a set of monocomponent oscillations which are matched in frequency need to be identified such that phase synchrony between two common oscillatory mode can be determined. To this end, we introduce a multivariate extension of the method proposed in [18], with the aim to obtain a set of multivariate monocomponent signals based on the bandwidth of the original multivariate signal. The first step is to partition the time-frequency plane into $2^l$ equal-width frequency bands, between the frequency range

$$\omega_{l,m} = \left[\frac{m}{2^{l+1}}, \frac{m+1}{2^{l+1}}\right] \tag{5}$$

where $l = 0,\dots,L$, is referred to as the *level* of the frequency bands and $m = 0,\dots,2^l-1$, the *index* of the frequency band. For a given frequency band $\omega_{l,m}$ at level $l$ and index $m$, the multivariate bandwidth $\mathbf{B}_{l,m}$ can then be calculated [19], as shown in Fig. 1.

To obtain the multivariate bandwidth within the frequency band $\omega_{l,m}$, we first calculate the Fourier transform of the inverse of the SST coefficients within the frequency band $\omega_{l,m}$, that is

$$\mathbf{\Phi}_{l,m}(\omega) = \left[\mathscr{F}\left\{R_\psi^{-1}\sum_{\omega\in\omega_{l,m}} T_n(\omega,b)\right\}\right]_{n=1,2} \tag{6}$$

[1]The detailed implementation of the SST can be found in [17].

where $n$ is the channel index, $\mathscr{F}\{\cdot\}$ the Fourier transform, $R_\psi$ the normalization constant [13] and $\mathbf{\Phi}_{l,m}(\omega) \in \mathbb{R}^N$ a column vector. The joint analytic spectrum is determined according to

$$S_{l,m}(\omega) = \frac{1}{E}||\mathbf{\Phi}_{l,m}(\omega)||^2 \tag{7}$$

where $E$ corresponds to the total energy of the joint analytic spectrum

$$E = \frac{1}{2\pi}\int_0^\infty ||\mathbf{\Phi}_{l,m}(\omega)||^2 \,\mathrm{d}\omega. \tag{8}$$

The joint global mean frequency is given by

$$\overline{\omega}_{l,m} = \frac{1}{2\pi}\int_0^\infty \omega S_{l,m}(\omega)\,\mathrm{d}\omega, \tag{9}$$

and corresponds to the average frequency of the joint analytic spectrum. The multivariate bandwidth squared (joint global second central moment [19]) measures the spectral deviation of the joint analytic spectrum from the joint global mean frequency, and is given by

$$\mathbf{B}_{l,m}^2 = \frac{1}{2\pi}\int_0^\infty (\omega - \overline{\omega}_{l,m})^2 S_{l,m}(\omega)\,\mathrm{d}\omega. \tag{10}$$

For illustration, consider a frequency band $\omega_{l,m}$ that contains two monocomponent signals separated in frequency, such that the frequency subbands $\omega_{l+1,2m}$ and $\omega_{l+1,2m+1}$ contain the separate monocomponent signals. From (10) the multivariate bandwidth in the frequency band $\omega_{l,m}$, is greater than the multivariate bandwidths within the individual subbands $\omega_{l+1,2m}$ and $\omega_{l+1,2m+1}$; implying that monocomponent signals separated in frequency can be identified by splitting larger frequency bands into smaller frequency subbands, based on the multivariate bandwidth [18]. In this way, a frequency band $\omega_{l,m}$ is split based on the following condition

$$\mathbf{B}_{l,m} > \frac{\mathbf{B}_{l+1,2m}\Lambda_{l+1,2m} + \mathbf{B}_{l+1,2m+1}\Lambda_{l+1,2m+1}}{\Lambda_{l+1,2m} + \Lambda_{l+1,2m+1}} \tag{11}$$

where

$$\Lambda_{l+1,2m} = \sum_{b=1}^{T}(A_{l+1,2m}(b))^2$$

$$\Lambda_{l+1,2m+1} = \sum_{b=1}^{T}(A_{l+1,2m+1}(b))^2$$

with $A_{l+1,2m}(b)$ and $A_{l+1,2m+1}(b)$ corresponding to the multivariate instantaneous amplitudes for the respective frequency subbands, given by

$$A_{l,m}(b) = \sqrt{\sum_{\omega\in\omega_{l,m}} |T_1(\omega,b)|^2 + \sum_{\omega\in\omega_{l,m}} |T_2(\omega,b)|^2}.$$

The condition in (11) considers the power differences between two frequency subbands, as frequency subbands that have negligible signal content would affect the outcome of whether or not the frequency band is split. The final set of $K$ frequency bands is given by $\{\omega_k\}_{k=1,\ldots,K}$.

Upon identifying the frequency bands $\{\omega_k\}_{k=1,\ldots,K}$, the instantaneous phase $\phi_k^n(b)$ for each frequency band $k$, and signal $n$, can now be calculated as

$$a_k^n(b)e^{i\phi_k^n(b)} = R_\psi^{-1}\sum_{\omega\in\omega_k} T_n(\omega,b). \tag{12}$$

The phase synchrony for each (outlined in Section 3) scale is then determined, and the phase symphony spectrogram can be calculated using e.g. the method in [9].

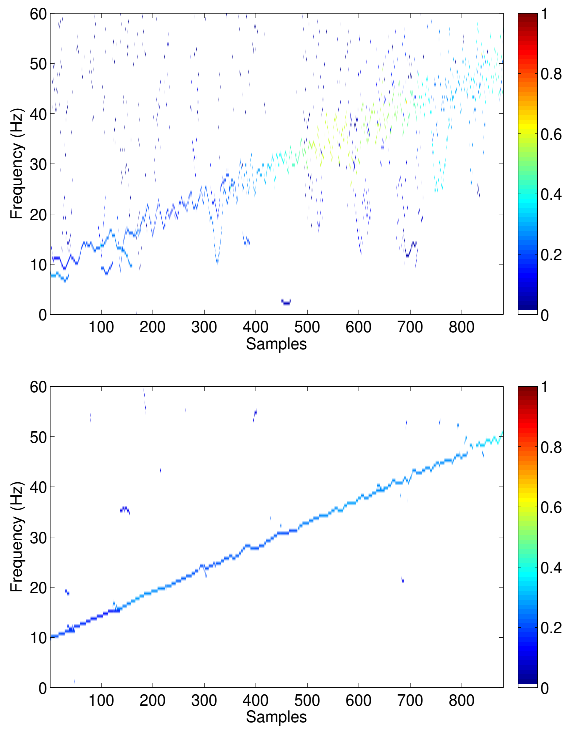


**Fig. 2**: Phase synchrony spectrograms of a bivariate linear chirp signal in white noise. (Upper panel) BEMD based phase synchrony method; (Lower panel) multivariate SST based phase synchrony method.

## 5. SIMULATIONS

Simulations were conducted on both synthetic and real world signals. The proposed method was compared to the bivariate empirical mode decomposition (BEMD) based phase synchrony method, as outlined in [9].

### 5.1. Synthetic signals

In order to quantify the performance of the proposed method, the first simulation was conducted on a bivariate signal containing a common sinusoidal oscillation of frequency $f_o$ in varying levels of Gaussian noise. The oscillations were sampled at $f_s = 256$Hz for a duration of 5 seconds. To assess the performance of the proposed multivariate SST based method, the average synchrony score $\rho_s$ was obtained at the frequency of the sinusoidal oscillation $f_o$. From Table 1, it can be seen that, as desired, synchrony scores observed for the proposed method are higher than the BEMD based phase synchrony method.

**Table 1**: The average synchrony, $\rho_s$, between the channels of a bivariate signal, at different frequency and noise levels.

| Algorithm | SNR \ Frequency | 5Hz | 10Hz | 20Hz | 40Hz |
|---|---|---|---|---|---|
| SST | 5dB | 0.88 | 0.81 | 0.58 | 0.25 |
| BEMD | 5dB | 0.44 | 0.25 | 0.15 | 0.06 |
| SST | 3dB | 0.8 | 0.71 | 0.42 | 0.14 |
| BEMD | 3dB | 0.34 | 0.17 | 0.11 | 0.03 |
| SST | 0dB | 0.75 | 0.62 | 0.29 | 0.08 |
| BEMD | 0dB | 0.29 | 0.13 | 0.07 | 0.02 |

To illustrate the performance advantages of using the multivariate SST based synchrony method in analyzing synchronized time-varying oscillations, the proposed method was next applied to a bivariate chirp signal sampled at $f_s = 256$Hz, in 5dB of white Gaussian noise. From Fig. 2 it can be seen that the proposed method localizes the chirp signal and eliminates most of the background noise. Also note the improvement over the BEMD based synchrony method.

### 5.2. Human motion analysis

The bivariate signal was obtained from two 3D accelerometers, attached to the wrists of a test subject. The subject was instructed to walk, with information pertaining to the arm swings being recorded by the accelerometers, our assumption was that the motion from the subject's left and right wrists was synchronized. The bivariate signal was constructed using the y-axis accelerometer data (the y-axis of the accelerometer was perpendicular to ground, when the subject was at rest) from the left and right wrists of the test subject.

Observe from Fig. 3a that the oscillations between the samples 400-800 and 900-1200 corresponding to the subject's arm swings appear to be phase locked. This is confirmed in Fig. 3b where both the multivariate SST (lower panel) and BEMD (upper panel) based phase synchrony spectrograms show intermittent phase synchronization at approximately 3Hz and 6Hz. Notice that the synchrony spectrogram of proposed method, localizes the phase synchronization more effectively with less variability and residual noise, compared with the BEMD based phase synchrony method.

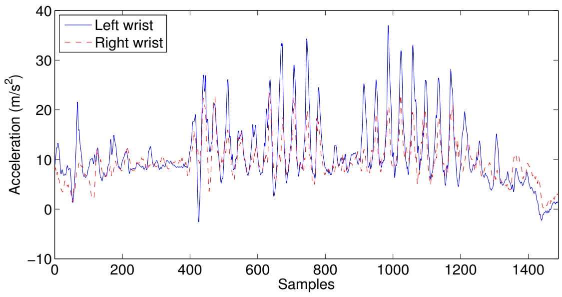


(a) Accelerometer data

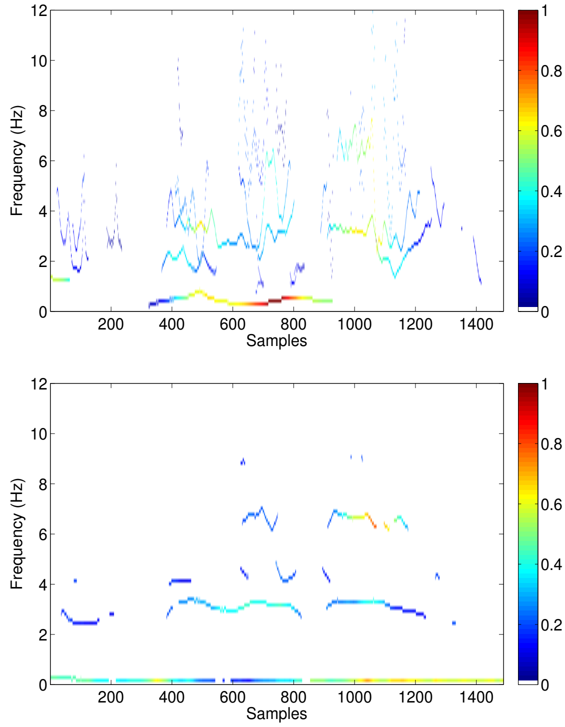


(b) Phase synchrony spectrograms

**Fig. 3**: Phase synchrony in human walk. (a) Time domain representation of the accelerometer data. (b) Phase synchrony spectrograms of the accelerometer data using (upper panel) BEMD based phase synchrony method and (lower panel) multivariate SST based phase synchrony method.

## 6. CONCLUSION

A robust phase synchrony measurement technique has been proposed using the synchrosqueezing transform. This is achieved by partitioning the time-frequency domain in such a way that a set of matched monocomponent signals can be identified and the phase synchrony estimated. The benefits of the proposed multivariate SST based phase synchrony method have been illustrated on both synthetic and real-world signals.

## 7. REFERENCES


[1] R. Q. Quiroga, A. Kraskov, T. Kreuz, and P. Grassberger, “Performance of different synchronization measures in real data: A case study on electroencephalographic signals,” *Physical Review E*, vol. 65, no. 4, 2002.

[2] E. Shane, C. Hughes, S. Olhede, and J. Toole, “Coherence of western boundary pressure at the rapid wave array: Boundary wave adjustments or deep western current convection?” *Journal of Physical Oceanography*, vol. 43, pp. 744–765, 2013.

[3] F. Varela, J.-P. Lachaux, E. Rodriguez, and J. Martinerie, “The brainweb: Phase synchronization and large-scale integration,” *Nature Reviews Neuroscience*, vol. 2, no. 4, pp. 229–239, 2001.

[4] C. Park, D. Looney, N. Rehman, A. Ahrabian, and D. P. Mandic, “Classification of motor imagery BCI using multivariate empirical mode decomposition,” *IEEE Transactions on Neural Systems and Rehabilitation Engineering*, vol. 21, no. 1, pp. 10–22, 2013.

[5] P. Tass, M. G. Rosenblum, J. Weule, J. Kurths, A. Pikovsky, J. Volkmann, A. Schnitzler, and H.-J. Freund, “Detection of n:m phase locking from noisy data: Application to magnetoencephalography,” *Physical Review Letters*, vol. 81, no. 15, pp. 3291–3294, 1998.

[6] A. Ahrabian, C. Took, and D. Mandic, “Algorithmic trading using phase synchronization,” *IEEE Journal of Selected Topics in Signal Processing*, vol. 6, no. 4, pp. 399–404, 2012.

[7] N. Huang, Z. Shen, S. Long, M. Wu, H. Shih, Q. Zheng, N. Yen, C. Tung, and H. Liu, “The Empirical Mode Decomposition and the Hilbert spectrum for nonlinear and non-stationary time series analysis,” *Proceedings of the Royal Society A*, vol. 454, pp. 903–995, 1998.

[8] C. M. Sweeny-Reed and S. J. Nasuto, “A novel approach to the detection of synchronisation in EEG based on empirical mode decomposition,” *Journal of Computational Neuroscience*, vol. 23, no. 1, pp. 79–111, 2007.

[9] D. Looney, C. Park, P. Kidmose, M. Ungstrup, and D. P. Mandic, “Measuring phase synchrony using complex extensions of EMD,” *Proceedings of the IEEE/SP 15th Workshop on Statistical Signal Processing (SSP 09)*, pp. 49–52, 2009.

[10] G. Rilling, P. Flandrin, P. Goncalves, and J. M. Lilly, “Bivariate empirical mode decomposition,” *IEEE Signal Processing Letters*, vol. 14, no. 12, pp. 936–939, 2007.

[11] D. Mandic, N. Rehman, Z. Wu, and N. Huang, “Empirical mode decomposition-based time-frequency analysis of multivariate signals: The power of adaptive data analysis,” *IEEE Signal Processing Magazine*, vol. 30, no. 6, pp. 74–86, 2013.

[12] C. Park, D. Looney, P. Kidmose, M. Ungstrup, and D. P. Mandic, “Time-frequency analysis of EEG asymmetry using bivariate empirical mode decomposition,” *IEEE Transactions on Neural Systems and Rehabilitation Engineering*, vol. 19, no. 4, pp. 366–373, 2011.

[13] I. Daubechies, J. Lu, and H.-T. Wu, “Synchrosqueezed wavelet transforms: An empirical mode decomposition-like tool,” *Applied and Computational Harmonic Analysis*, vol. 30, no. 2, pp. 243–261, 2011.

[14] F. Auger, P. Flandrin, Y. Lin, S. McLaughlin, S. Meignen, T. Oberlin, and H. Wu, “Time-frequency reassignment and synchrosqueezing: An overview,” *IEEE Signal Processing Magazine*, vol. 30, no. 6, pp. 32–41, 2013.

[15] R. Carmona, W.-L. Hwang, and B. Torrésani, *Practical time-frequency analysis*. Academic Press, 1998.

[16] H.-T. Wu, P. Flandrin, and I. Daubechies, “One or two frequencies? The synchrosqueezing answers,” *Avanced Adaptive Data Analysis*, vol. 3, no. 1, pp. 29–39, 2011.

[17] G. Thakur, E. Brevdo, N. S. Fuckar, and H.-T. Wu, “The synchrosqueezing algorithm for time-varying spectral analysis: Robustness properties and new paleoclimate applications,” *Signal Processing*, vol. 93, no. 5, pp. 1079–1094, 2013.

[18] S. Olhede and A. Walden, “The Hilbert spectrum via wavelet projections,” *Proceedings of the Royal Society A*, vol. 460, pp. 955–975, 2004.

[19] J. M. Lilly and S. C. Olhede, “Bivariate instantaneous frequency and bandwidth,” *IEEE Transactions on Signal Processing*, vol. 58, no. 2, pp. 591–603, 2010.